# 8-Oxoguanine DNA glycosylase-1-mediated DNA repair is associated with Rho GTPase activation and α-smooth muscle actin polymerization

Jixian Luo [a,1], Koa Hosoki [b,2], Attila Bacsi [a,3], Zsolt Radak [a,4], Muralidhar L. Hegde [c,5], Sanjiv Sur [b,d], Tapas K. Hazra [b,d], Allan R. Brasier [c,d], Xueqing Ba [a,6], Istvan Boldogh [a,d,*]

[a] Department of Microbiology and Immunology, University of Texas Medical Branch at Galveston, Galveston, TX 77555, USA

[b] Department of Internal Medicine, University of Texas Medical Branch at Galveston, Galveston, TX 77555, USA

[c] Department of Biochemistry and Molecular Biology, University of Texas Medical Branch at Galveston, Galveston, TX 77555, USA

[d] Sealy Center for Molecular Medicine, University of Texas Medical Branch at Galveston, Galveston, TX 77555, USA

[*] Corresponding author at: University of Texas Medical Branch at Galveston, Departments of Microbiology and Immunology, 301 University Blvd, Medical Research Building, Galveston, Texas 77555-1070, United States. Fax: + 1 409 747 6869. E-mail address: sboldogh@utmb.edu (I. Boldogh).

[1] Present address: School of Life Science, Shanxi University, Taiyuan, China.

[2] Present address: Institute for Clinical Research, Mie National Hospital, Mie, Japan.

[3] Present address: Department of Immunology, Medical and Health Science Center, University of Debrecen, Debrecen, Hungary.

[4] Present address: Research Institute of Sport Science, Semmelweis University, Budapest, Hungary.

[5] Present address: Radiation Oncology, Houston Methodist Research Institute, Houston, TX, USA.

[6] Present address: Key Laboratory of Molecular Epigenetics, Institute of Genetics and Cytology, Northeast Normal University, Changchun, China.

**Abbreviations:** 8-oxoG, 8-oxo-7,8-dihydroguanine; 8-oxodG, 8-oxo-7,8-dihydro-2'-deoxyguanosine; α-SMA, -smooth muscle actin; Ab, antibody; BER, base excision repair; FU, fluorescence unit; FapyG, 2,6-diamino-4-hydroxy-5-formami-dopyrimidine; GEF, guanine nucleotide exchange factor; GOx, glucose oxidase; GST, glutathione S-transferase; $^{Mant}$GTP, 2'-(or-3')-O-(N-methylanthraniloyl)guanosine 5'-triphosphate; $^{Mant}$GDP, 2'-(or-3')-O-(N-methylanthraniloyl)guanosine 5'-diphosphate; OGG1, 8-oxoguanine DNA glycosylase-1; ROS, reactive oxygen species

## Abstract

Reactive oxygen species (ROS) are activators of cell signaling and modify cellular molecules, including DNA. 8-Oxo-7,8-dihydroguanine (8-oxoG) is one of the prominent lesions in oxidatively damaged DNA, whose accumulation is causally linked to various diseases and aging processes, whereas its etiological relevance is unclear. 8-OxoG is repaired by the 8-oxoguanine DNA glycosylase-1 (OGG1)-initiated DNA base excision repair (BER) pathway. OGG1 binds free 8-oxoG and this complex functions as an activator of Ras family GTPases. Here we examined whether OGG1-initiated BER is associated with the activation of Rho GTPase and mediates changes in the cytoskeleton. To test this possibility, we induced OGG1- initiated BER in cultured cells and mouse lungs and used molecular approaches such as active Rho pull- down assays, siRNA ablation of gene expression, immune blotting, and microscopic imaging. We found that OGG1 physically interacts with Rho GTPase and, in the presence of 8-oxoG base, increases Rho–GTP levels in cultured cells and lungs, which mediates α-smooth muscle actin (α-SMA) polymerization into stress fibers and increases the level of α-SMA in insoluble cellular/tissue fractions. These changes were absent in cells lacking OGG1. These unexpected data and those showing that 8-oxoG repair is a lifetime process suggest that, via Rho GTPase, OGG1 could be involved in the cytoskeletal changes and organ remodeling observed in various chronic diseases.

**Keywords**: ROS, OGG1, Base excision repair, Rho–GTP, Cytoskeleton, Free radicals

Oxidative stress is generated by multiple exogenous agents and endogenous sources in mammalian cells. The resulting reactive oxygen species (ROS) cause damage to cellular molecules, includ- ing DNA [1]. In DNA guanine is a primary ROS target because it has the lowest reduction potential among the nucleic acid bases [2]; 8-oxo-7,8-dihydroguanine (8-oxoG) is thus one of the most abundant base lesions. Because of its potential to pair with adenine, 8-oxoG is also one of the most mutagenic DNA lesions among over 20 identified oxidative modifications to guanine [3,4]. Accumula- tion of 8-oxoG in DNA has been linked to various inflammatory diseases, as well as aging processes [5]. The oxidatively damaged bases are preferentially repaired by the base excision repair (BER) pathway [6,7], which utilizes glycosylases to excise the lesion via cleaving its N-glycosidic bond, followed by endonucleolytic cleavage and subsequent gap-filling [6,8].

8-Oxoguanine DNA glycosylase-1 (OGG1) is the key enzyme in removing 8-oxoG and 2,6-diamino-4-hydroxy-5-formamidopyri- midine (FapyG) from DNA with equal specificity and kinetics during BER to prevent mutations and maintain genomic integrity [6,9,10]. Surprisingly, Ogg1-knockout (KO) mice have no particular phenotype; their life span is unaltered, showing only a moderate predisposition to tumorigenesis, despite increased genomic 8-oxoG levels [11–13]. A lack of OGG1 activity in KO mice resulted in increased resistance to inflammation [14], changes in whole-body energy homeostasis, increased susceptibility to obesity, and metabolic dysfunction [15]. These results suggest additional, not yet defined functions of OGG1 protein and/or its repair

product, 8-oxoG. In support of this hypothesis, accumulating data suggest that OGG1 may play roles in multiple cellular processes. For example, it has been shown that OGG1 colocalizes with centrioles (microtubule organizing centers), microtubule networks, and mitotic chromosomes [16,17]. It has also been shown that OGG1-generated free 8-oxoG base binds to OGG1 and increases its β-lyase activity, mediating product-assisted catalysis in an enzyme-catalyzed reaction [18]. Our recent studies also showed that 8-oxoG binds cytoplasmic OGG1, and the OGG1 8-oxoG complex acts as a guanine nucleotide exchange factor (GEF) catalyzing the exchange of GDP with GTP to promote activation of Ras and Rac1 small GTPases [19–21].

In response to DNA damage, or in DNA damage-induced senescent cells, reorganization of the cytoskeleton, actin filaments (stress fibers), and filopodia has been observed [22], although the molecular events directly responsible for these cytoskeletal mor- phological changes are not yet well defined. Among the small GTPase family members, activation of the Ras homology (Rho) proteins RhoA, RhoB, and RhoC has been shown to regulate many aspects of intracellular actin dynamics, including stress fiber formation [23]. Taking into account that OGG1 functions as a GEF when complexed with 8-oxoG [19–21], we hypothesized that OGG1-BER is associated with Rho activation and transient morphological changes in ROS-exposed cells. Here we show that OGG1-initiated repair of oxidative DNA damage was followed by an increase in Rho–GTP levels and stress fiber formation in cultured cells and lung tissues. Thus our studies establish a link between repair of oxidatively altered guanine and changes in

cellular architecture, placing OGG1 at the center of a complex signaling network.

## Materials and methods

### *Materials*

8-OxoG (Cat. No. 89290) was from Cayman Chemical Co. (Ann Arbor, MI, USA); FapyG was a kind gift from Dr. Miral Dizdaroglu (National Institute of Standards and Technology, Gaithersburg, MD, USA); glucose oxidase from Aspergillus niger (GOx; Cat. No. G7141-10KU), FITC-conjugated phalloidin (Cat. No. P5282-.1MG), trietha- nolamine (TEA; Cat. No. 90279-100ML), and N-TER Nanoparticle siRNA Transfection System (Cat. No. N2913) were from Sigma–Aldrich (St. Louis, MO, USA); rabbit polyclonal antibody (Ab) to α-smooth muscle actin (anti-α-SMA; Cat. No. ab5694) was from Abcam (Cambridge, MA, USA); monoclonal Abs to glyceral-dehyde-3-phosphate dehydrogenase (GAPDH; Cat. No. 2118S) and α-tubulin (Cat. No. 3873S) were from Cell Signaling Technology (Danvers, MA, USA); active Rho pull-down and detection kit (Cat. No. 16116Y) was from Thermo Scientific Pierce Biotechnology (Rockford, IL, USA); OGG1 rabbit monoclonal Ab (Cat. No. 5104-1) was from the Abcam subsidiary Epitomics (Burlingame, CA, USA). siGENOME SMARTpool for human OGG1 (Cat. No. M-005147-03) was from Dharmacon Thermo Scientific (Pittsburgh, PA, USA). Rho activator (calpeptin, Cat. No. CN01) and Rho inhibitor (C3 transferase, Cat. No.

CT04) were from Cytoskeleton (Denver, CO, USA); His-tagged RhoA protein (Cat. No. NBP1-50933) was from Novus Biologicals (Littleton, CO, USA); and OGG1 protein was a kind gift from Dr. Hazra (Department of Biochemistry & Molecular Biology, UTMB, Galveston, TX, USA). 2′-(or-3′)-O-(N-methylanthraniloyl) guanosine 5′-triphosphate ($^{Mant}$GTP) and 2′-(or-3′)-O-(N-methy- lanthraniloyl) guanosine 5′-diphosphate ($^{Mant}$GDP) were from Cytoskeleton.

*Cell culture*

Human diploid fibroblast (MRC5) and mouse embryonic fibroblast (MEF) cells were maintained in Earle's minimum essential medium and Dulbecco's modified Eagle's medium/F-12 (Ham) supplemented with 10% fetal bovine serum (FBS), glutamine, penicillin, and streptomycin; cells were grown at 37 °C in 5% $CO_2$, starved in 0.5% FBS medium for 24 h, and starved in FBS-free medium for 16 h before Rho activation. 8-OxoG (10 μM) or GOx (100 ng/ml) was added to cells in serum-free medium, and cell extracts were made at the indicated times after 8-oxoG or GOx addition.

*Animals*

Animal experiments were performed according to the National Institutes of Health guidelines for the use of experimental animals and approved by the University of Texas Animal Care and Use Committee (Protocol 0807044A). Eight-week-old female BALB/c mice (The Jackson Laboratory, Bar Harbor, ME, USA) were challenged intranasally with 1 μM 8-oxoG (60 ml) or an equal volume of vehicle and sacrificed, and the lungs were excised [24]. In other experiments, mice were directly sacrificed without treatment.

*Histology and immunohistochemistry*

For immunochemistry histology staining of α-SMA or F-actin, mice were challenged with 1 μM 8-oxoG (in 60 ml phosphate- buffered saline; PBS) and sacrificed after 30 min. Mouse lungs were fixed, sectioned (4 μm), and stained with α-SMA Ab and/or FITC–phalloidin. Cells on chambers slides were challenged with the OGG1-initiated BER by-product 8-oxoG for 20 min and after treatment fixed with 4% paraformaldehyde for 20 min at room temperature, then washed twice with wash buffer (0.05% Tween 20 in PBS), and permeabilized with 0.1% Triton X-100 for 3 min. After the wash, blocking solution (1% bovine serum albumin in 0.05% Tween 20 in PBS) was added for 30 min. Mouse anti-rabbit α-SMA monoclonal Ab and FITC–phalloidin were diluted in the blocking solution. After 1 h incubation with the primary Ab (1:300) followed by three washes with washing buffer, the secondary Ab (goat

anti-mouse, FITC-conjugated, dilution 1:500) was added for 30–60 min. Cells were washed with 0.05% Tween 20 in PBS three times, dried, and mounted in antifade reagent (Cat. No. S3023 from Dako North America, Carpinteria, CA, USA). Stress fibers were visualized under a microscope using FITC-conjugated phalloidin (50 μg/ml) per the manufacturer's protocol, at 600 x magnification. Each image shown was a typical one in the field of view.

*Assessment of active Rho levels*

Assessment of Rho–GTP levels in cells was conducted using the active Rho pull-down assay kit as recommended by the manufacturer and described previously [19,20]. Briefly, cells were challenged with 100 ng/ml GOx or 10 μM 8-oxoG at 37 °C for the indicated times and lysed in 25 mM Tris–HCl, pH 7.5, 150 mM NaCl, 60 mM $MgCl_2$, 1% Nonidet P-40, and 5% glycerol, and Rho–GTP in 500 μg extracts was captured by the GST–Rho-binding domain of Rhotekin immobilized to glutathione resin [25]. After being washed with binding buffer, the activated Rho (Rho–GTP) was eluted with Laemmli buffer (0.125 M Tris–HCl, 4% SDS, 20% glycerol, 10% 2-mercaptoethanol, pH 6.8) and quantified by Western blot assay using ImageJ 1.46R.

To assess Rho–GTP levels in the lung lysate, mouse lungs were excised and homogenized in lysis buffer provided by the manufacturer (Thermo Scientific Pierce Biotechnology) containing 10 mM EDTA and 60 mM $MgCl_2$. 8-OxoG (10 μM) was added to 500 μg lung extracts and incubated at 37 °C for the

indicated times. In other experiments, mice were challenged intranasally with 1 μM 8-oxoG (60 ml) for 30 min and sacrificed and mouse lungs were homogenized. Rho–GTP in 500 μg lung extracts was captured and quantified by Western blot analysis.

*Protein–protein binding assays*

To determine the interactions between OGG1 and Rho, we conducted His-affinity pull-down assays as previously described, with slight modification [19]. Briefly, nickel–nitrilotriacetic acid (Ni–NTA)-agarose beads (Qiagen, Valencia, CA, USA) were mixed with His-RhoA protein (6 pmol) in 300 ml of interaction buffer (50 mM $NaH_2PO_4$, 300 mM NaCl, 20 mM imidazole, 0.05% Tween 20, pH 7.5). After a 30-min incubation at 4 °C, His-RhoA-bound beads were washed three times, and an equimolar amount of OGG1 (6 pmol), alone or plus 8-oxoG (6 pmol), was added to the interaction buffer. Samples were incubated for 30 min at 4 °C, washed twice with interaction buffer, and eluted with Laemmli buffer at 100 °C for 5 min. The eluents were analyzed on Western blots.

*Guanine nucleotide exchange assay*

GDP–GTP and GTP–GDP exchange on RhoA was determined by real-time fluorescence spectroscopic analysis [21,26]. Specifically, RhoA (6 pmol) was loaded with the nucleotide analog $^{Mant}GTP$ or $^{Mant}GDP$ in exchange buffer

containing 20 mM Tris (pH 7.5), 150 mM NaCl, 1 mM dithiothreitol, 50 mg of bovine serum albumin for 30 min. In the case f GDP–GTP exchange, RhoA–$Mant_{GDP}$ and OGG1 protein (6 pmol) + 8-oxoG base (6 pmol) were mixed with untagged GTP. A similar strategy was used to monitor GTP–GDP exchange. Kinetic changes in the fluorescence of RhoA–$Mant_{GDP}$ or RhoA–$Mant_{GTP}$ were determined using a POLARstar Omega reader (BMG Labtech, Ortenberg, Germany). Curves were fitted using MS Excel. The half-life of RhoA–$Mant_{GDP}$ was determined using POLARstar Omega software.

*Preparation of soluble and insoluble cellular fractions*

Cells were lysed in Triton X-100 buffer (50 mM Tris, pH 7.5, 1 mM EDTA, 1 mM EGTA, 1 mM $Na_3VO_4$, 5 mM sodium pyrophosphate, 10 mM sodium glycerophosphate, 1% Triton X-100, 50 mM NaF plus 1% protease inhibitor cocktail) and lysates were assayed for protein concentration using the Bradford reagent and then diluted with 2 x Laemmli loading buffer for SDS–PAGE. The pellets from cell lysates (Triton X-100-insoluble α-SMA pool) were sonicated in 2 x loading buffer before processing for SDS–PAGE [27]. Equal amounts of protein were then loaded onto 4–20% Tris– glycine gels and electrophoresed for 90 min at 300 mA constant current. Proteins were blotted onto membranes by electrophoretic transfer at 100 V for 1 h at 4 $^{o}$C and α-SMA levels determined by Western blotting.

*Isolation of stress fibers*

Cells were cultured for 1 day in 100-mm dishes and starved in 0.5% FBS-containing medium for 16 h before challenge with 8-oxoG base. Stress fibers were isolated as previously described, with slight changes [28]. Briefly, cells were washed in ice-cold PBS and then treated with a low-ionic-strength extraction solution consisting of 2.5 mM TEA (pH 8.2) with protease inhibitor cocktail at 4 °C with gentle agitation for 10–40 min, until the dorsal side of the cell became free-floating. Cells were then treated with extraction buffer I (0.05% NP-40, 1% protease inhibitor cocktail in PBS, pH 7.2) for 5 min. At this stage some cells still had the dorsal side and/or the nucleus, which were then removed by gentle shearing under a phase-contrast microscope with a stream of extraction buffer I. The material still attached to culture dishes was gently washed in extraction buffer II (0.5% Triton X-100, 10% protease inhibitor cocktail in PBS, pH 7.2). The extracted material was scraped off from the dish and suspended in extraction buffer II, and the crude stress fiber isolates were suspended in PBS contain- ing protease inhibitor cocktail, pH 7.4) and centrifuged at 100,000 g for 1 h. The pellet containing highly concentrated stress fibers was sonicated in SDS loading buffer and analyzed by Western blot analysis.

*SiRNA ablation of gene expression*

Cells at 60% confluence were transfected with OGG1 siRNA or control siRNA (at 20 nM, as determined in preliminary studies) using the N-TER Nanoparticle siRNA Transfection System. After 24 h, cells were retransfected for another 36 h as we described previously [21]. The efficiency of OGG1 depletion was determined at the protein level by Western blotting.

*Statistical analyses*

Values are presented as means ± SEM. Statistical comparisons of differences were performed using one-way ANOVA combined with t tests; $p < 0.05$ was considered statistically significant by Origin 9.

**Results**

*OGG1-BER-associated increases in level of GTP-bound Rho in cultured cells and mouse lungs*

To test for a link between repair of oxidative DNA damage and the activation of Rho GTPases, cells were exposed to GOx, which has been reported to increase intracellular ROS levels and oxidative DNA damage [29]. Cell extracts were made and Rho–GTP levels were determined by active Rho pull-down assays. Our results showed that Rho–GTP levels had bipartite peaks, at 5 min and then

at 30 min, in both MRC5 and MEF cells after exposure to GOx (Fig. 1A and B, respectively). To examine whether OGG1-BER has a role in Rho activation OGG1 expression was downregulated, followed by GOx exposure. Intriguingly, compared to control we observed no increase in Rho–GTP levels in extracts made from OGG1-depleted cells (Fig. 1C), suggesting an important role for OGG1-initiated BER and/or OGG1 in oxidative stress-induced Rho activation.

To examine the impact of OGG1-initiated repair of oxidative DNA damage and rule out multiple effects of ROS, we challenged cells with 8-oxoG base. Challenging MRC5 and MEF cells with 8-oxoG resulted in activation of Rho GTPase (between 2.5 and 20 min; Fig. 1D and E), suggesting that 8-oxoG challenge mimics OGG1-initiated repair of oxidatively damaged DNA. OGG1 excises 8-oxoG and FapyG from DNA with equal specificity and kinetics [3,4]. Therefore, we challenged cells with FapyG. As shown in Fig. 1F, FapyG failed to increase GTP-bound levels of Rho, whereas positive 8-oxoG and calpeptin (a Rho activator) did so. Similarly, 8-oxo-deoxyguanosine (8-oxodG) failed to activate Rho GTPase, in line with its inability to activate Ras and Rac family GTPases [19,21]. To determine the percentage of Rho–GTP, autoradiograms were quantified using ImageJ software. In mock-exposed cells the calculated percentages of activated Rho were 1.06 and 1.45% (in MRC5 and MEF, respectively) upon 8-oxoG treatment; its levels were between 3.8 and 7.3% in MRC5 cells (Fig. 1D, bottom) and 2.8 and 8.2% in EF cells (Fig. 1E, bottom). Importantly, 8-oxoG- induced increases in Rho–GTP levels were similar to those mediated by oxidative stress (GOx) (Fig. 1A and B, bottom).

To further examine the role of OGG1 in 8-oxoG-mediated Rho activation, cells were depleted of OGG1 by siRNA and then challenged with 8-oxoG. Our results showed that a > 80% OGG1 depletion (Fig. 1G, inset) nearly prevented 8-oxoG exposure-induced Rho activation in MRC5 cells (Fig. 1G). In support, 8-oxoG challenge rapidly increased Rho–GTP level in $Ogg1^{+/+}$, but not in $Ogg1^{-/-}$ MEF cells (Fig. 1H).

To test whether Rho is activated in an organ/tissue environment as a consequence of OGG1-initiated BER, we challenged mice with 8-oxoG for 30 min and active Rho pull-down assays were undertaken. Results in Fig. 1I show increased levels of Rho–GTP in individual mouse lungs. Owing to limitations in keeping a time course, we generated extracts from unchallenged lungs and then added 8-oxoG. Our results showed that adding 8-oxoG base to lung extracts induced a rapid increase in GTP-bound Rho levels (Fig. 1J). The percentage changes in Rho–GTP in 8-oxoG-treated lung extracts (Fig. 1J, bottom) were similar to those observed in cell culture (Fig. 1A, B, D, and E), suggesting that in the presence of 8-oxoG base OGG1 in the extracts activates Rho.

Expression levels of RhoA, RhoB, and RhoC vary significantly depending on cell/tissue type [30]. Utilizing isotype-specific Abs, we observed that in both MRC5 and MEF cells, RhoA is the most abundant among the three family members (Fig. 1K), strongly suggesting that the observed increase in Rho–GTP levels is primarily represented by RhoA. Together, these data suggest that Rho activation requires OGG1 when cells are exposed to oxidative stress or 8-oxoG, a product of OGG1-initiated BER.

*Interaction of OGG1 with RhoA and GDP→GTP exchange*

Rho GTPases are inactive when GDP-bound and active when GTP-bound. Cycling between these states is controlled by three known classes of regulatory proteins: GTPase-activating proteins, guanine nucleotide dissociation inhibitors, and GEFs [31]. The rapid OGG1-dependent increase in Rho–GTP levels upon ROS or 8-oxoG exposure suggests that OGG1 promotes GDP → GTP exchange and may function as a GEF. To examine this possibility we first tested interactions between OGG1 and RhoA proteins. The results showed that the OGG1 protein physically interacts with RhoA (Fig. 2A). Addition of 8-oxoG base did not further increase OGG1 binding to RhoA (Fig. 2A). Furthermore, loading of RhoA with GTP or GDP had no effect on OGG1 7 8-oxoG binding to RhoA (Fig. 2B).

To test whether such binding could contribute to Rho activation, we examined the GDP → GTP exchange as previously described [21]. $^{Mant}$GDP's fluorescence intensity is 1.33 x $10^5$ fluorescence units (FU). When bound to RhoA, the fluorescence intensity was increased to 1.9 x $10^5$ FU. Upon addition of OGG1 plus 8-oxoG along with unlabeled GTP, the fluorescence intensity of RhoA–$^{Mant}$GDP rapidly decreased, indicating that the RhoA-bound $^{Mant}$GDP was replaced by nonfluorescent GTP. Fifty percent of $^{Mant}$GDP was replaced by GTP within 60 s. In controls without the 8-oxoG base, OGG1 plus GTP did not change RhoA–$^{Mant}$GDP fluorescence. Neither did 8-oxoG base plus GTP, with- out OGG1 (Fig. 2C).

Next, we examined whether OGG1 catalyzes GTP → GDP exchange. Similar to $Mant_{GDP}$, the fluorescence intensity of $Mant_{GTP}$ was increased (from 1.33 x $10^5$ to 1.9 x $10^5$ FU) when bound to RhoA. Upon addition of OGG1 plus 8-oxoG along with unlabeled GDP, there was no change in RhoA–$Mant_{GTP}$ fluorescence intensity, implying the absence of any guanine nucleotide exchange. OGG1 or 8-oxoG alone caused no change in RhoA–$Mant_{GTP}$ fluorescence in the presence of GDP (Fig. 2D). Together, these data suggest that OGG1 in complex with 8-oxoG functions as a guanine nucleotide exchange factor.

*OGG1-BER-associated α-SMA polymerization into stress fibers*

To explore the functional consequence of OGG1-BER-mediated activation of RhoA in a cellular context, changes in stress fiber levels were examined. To do so, we utilized serum-starved MRC5 and MEF cells to visualize cytoskeletal changes microscopically by using FITC–phalloidin. Microscopic imaging showed that in mock- treated cells the bound level of FITC–phalloidin was low. Importantly, exposure of cells to 8-oxoG induced obvious changes in the cytoskeleton, as shown by the appearance of stress fibers in both MRC5 and MEF cells (Fig. 3A). Furthermore, these changes were not observed in OGG1-knockout cells (Fig. 3A, lowest row), in line with the dependence on OGG1 in the 8-oxoG-induced increases in Rho–GTP levels (shown in Fig. 1I). As a positive control, the Rho activator calpeptin (1 unit/ml) induced formation of stress fiber in MRC5 cells and MEF (both $Ogg1^{+/+}$ and $Ogg1^{-/-}$). In addition to MRC5 and

MEF cells, human normal bronchial epithelial cells were also affected by 8-oxoG exposure, displaying stress fibers (Fig. 3B). This implies that not only fibroblasts, but also epithelial cells, respond to 8-oxoG and possibly to OGG1-initiated repair of oxidative DNA damage with cytoskeletal changes. Stress fibers that contain α-SMA generate more contractile force than do stress fibers that contain only β- and γ-cytoplasmic actin [32]. To test whether α-SMA level was increased in fibers, MRC-5 and MEF cells were exposed to 8-oxoG and analyzed by Western blotting. Our results showed that from 10 min on, the level of α-SMA was increased in stress fibers in MRC-5 and MEF cells (Fig. 3C and D), suggesting that α-SMA is incorporated into stress fibers in response to 8-oxoG exposure. In contrast, there was no obvious increase in α-SMA levels in the stress fibers of Ogg1 $^{-/-}$ MEFs in response to 8-oxoG (Fig. 3E). These results support the idea that OGG1-dependent Rho activation is the primary reason for α-SMA polymerization into stress fibers upon 8-oxoG addition.

To further explore the importance of OGG1 in activation of Rho and α-SMA polymerization, OGG1 was depleted from MRC5 cells via siRNA. Cells with decreased (~80%) OGG1 showed no obvious increase in α-SMA in stress fibers after exposure to 8-oxoG (Fig. 3F). To test whether Rho activation is the primary cause of stress fiber formation by 8-oxoG exposure, we utilized a Rho inhibitor (C3 transferase, 2 μg/ml), shown previously to prevent formation of stress fibers [33]. Preincubation of cells with C3 transferase significantly decreased the level of α-SMA in the stress fibers in Ogg1 $^{+/+}$ MEF cells (Fig. 3G). These data strongly suggest that 8-oxoG exposure-induced α-SMA incorporation into

stress fibers is OGG1-dependent, linking OGG1-initiated repair of oxidative DNA damage to cellular cytoskeletal changes.

*Cytoskeletal changes in mouse lungs upon 8-oxoG challenge*

Next we examined whether the cytoskeleton was changed in mouse lungs after 8-oxoG challenge. The lungs were challenged intranasally with 8-oxoG and then excised and sectioned (see Materials and methods). Microscopic imaging showed an increased colocalization of α-SMA with F-actin in subepithelial regions of lung bronchioles (Fig. 4A), suggesting that α-SMA is polymerized into the cytoskeleton in response to 8-oxoG. To confirm the incorporation of soluble α-SMA into stress fibers, lungs were homogenized and the Triton X-100-insoluble fractions isolated and subjected to immunoblotting. As shown in Fig. 4B, 8-oxoG challenge increased α-SMA levels in the Triton X-100-insoluble cytoskeletal fractions of mouse lungs.

Moreover, this increase was accompanied by a decrease in α-SMA levels in the soluble fraction. To validate the method used for this in vivo observation, MRC-5 cells were exposed to 8-oxoG and fractionated into Triton X-100-insoluble/soluble fractions similar to the lung tissue. Immunoblotting showed α-SMA redistribution into the insoluble fraction in response to 8-oxoG (Fig. 4C). These results imply that α-SMA is incorporated into Triton X-100-insoluble cytoskeletal fraction in response to 8-oxoG both in lungs and in cultured cells.

## Discussion

Supraphysiological levels of 8-oxoG in the genome have been linked to various diseases, including malignancies, aging-related neurological diseases, and aging processes themselves [34–38]. A common link among these processes is change in the actin cytoskeleton, cell–cell interactions, and extracellular matrix, and nearly all are thought to be etiologically linked to oxidative stress [39]. Here we show that only OGG1-expressing cells showed increased Rho activation and α-SMA polymerization into stress fibers in response to oxidative stress exposure of cells. Thus our data provide the first evidence for an association between OGG1-initiated repair of oxidative DNA damage and changes in cytoskeleton, which may be one among multiple mechanistic explanations for the link between OGG1-BER and aging as well as the development of diseases.

Our present study shows an OGG1 expression-dependent increase in Rho–GTP level upon oxidative stress exposure. Increases in Rho–GTP levels were biphasic; therefore we speculated that the immediate early peak could be due to ROS because Rho has a redox-sensitive motif containing two cysteine residues (GXXXCGK(S/T)C) in the phosphate-binding loop [40,41], whereas the second peak may be a result of OGG1-BER. To pursue the latter hypothesis we challenged cells with 8-oxoG, which increased levels of Rho–GTP only in OGG1-expressing cells, implying that both OGG1 and 8-oxoG base, one of the products of OGG1-BER, are important to Rho activation.

In theory, activation of Rho GTPases could occur through stimulation of a GEF or inhibition of GTPase activating factor; in practice, however, all evidence points to GEFs being the most critical mediators of Rho GTPase activation [42]; these have the ability to catalyze the exchange of GDP → GTP on Rho GTPases. Such actions of GEFs can be measured by their ability to stimulate nucleotide exchange in vitro [21]. To obtain initial information on the role of its GEF activity, we first examined OGG1's ability to bind RhoA in vitro. The OGG1 protein physically interacts with Rho protein. Interestingly, interactions between OGG1 and Rho did not require 8-oxoG base in vitro, which is different from the binding of OGG1 to Ras or Rac1 [19,21]. At this time, we have no information on in cellulo interactions between OGG1 and RhoA; however, the rapid activation of Rho upon OGG1-initiated BER, mimicked by the addition of the OGG1-BER product 8-oxoG base, strongly suggests their interaction. Furthermore, in the presence of 8-oxoG base, OGG1 efficiently catalyzed exchange of Rho–$^{Mant}$GDP with GTP. These results were not entirely surprising, as OGG1 plus 8-oxoG functions as guanine nucleotide release factor for canonical Ras family GTPases [19], whereas it has GEF activity for Rac1, as we showed previously [21]. In our experiments, substitution of $^{Mant}$GTP for unlabeled GTP was not detectable, suggesting that OGG1 primarily catalyzes GDP → GTP exchange. These data are consistent with those showing that during guanine nucleotide exchange, GEFs interact with GDP-bound GTPases and dissociate GDP at an increased rate, and the bound GTP then promotes the release of the GEF from the GTPase [43,44].

GEFs require posttranslational modifications to activate Rho GTPases [45,46]. In the case of OGG1, its repair product 8-oxoG base was required for GDP → GTP exchange. Indeed, a study showed that OGG1 binds the free 8-oxoG base with high affinity (binding constant ($K_d$) 0.56 ± 0.19 nM) [19]). OGG1's binding by 8-oxoG was necessary for activation of Ras and Rac1. It was thus unexpected that OGG1's binding by 8-oxoG was not necessary for interaction with Rho, but it was essential for Rho guanine nucleotide exchange. These results allow us to speculate that Rho-associated OGG1 binds 8-oxoG and then mediates GDP → GTP exchange. It has been shown that OGG1 excises not only 8-oxoG, but also FapyG, from DNA, with equal specificity and kinetics [4]. In view of these facts, we wondered if FapyG exposure of cells increased Rho–GTP levels. Results were negative. Lack of Rho activation by FapyG is consistent with data showing its undetectable binding to OGG1, which was previously analyzed by changes in OGG1's intrinsic tryptophan fluorescence [19].

Conventionally, Rho activation modulates the assembly of contractile actomyosin stress fibers, Rac–GTP produces lamellipodia and membrane ruffles, and Cdc42 induces filopodia formation [30]. To gain insight into the possible biological consequences of OGG1-BER-associated Rho activation, we examined changes in the α-SMA polymerization into stress fibers, a process primarily driven by RhoA–GTP. Our data show that activation of Rho by OGG1-BER, mimicked by the addition of 8-oxoG base, resulted in increased stress fiber content in both MRC5 and MEF fibroblasts, as shown first using microscopic

imaging. To build upon the imaging data, we showed an OGG1-dependent increase in levels of α-SMA in the insoluble cellular fractions.

ROS-induced signaling pathways are involved in distinct cellular biological processes, such as proliferation, cell–cell interactions, cell migration, (re)organization of intracellular filaments, and regulation of the extracellular matrix [39]. There is evidence that suitably activated fibroblasts can give rise to a differentiated phenotype characterized by the induction of α-SMA, which is incorporated into stress fibers, so the cells are aptly identified as myofibroblasts [47]. In our studies we primarily utilized fibroblast cells and carried out in vivo experiments, and demonstrated that ROS-induced DNA damage/repair-driven Rho activation converts fibroblasts to α-SMA-positive cells, which is one of the myofibroblast phenotypes. To circumvent implication of ROS in Rho activation and α-SMA polymerization into stress fibers, most of our studies utilized a specific product of OGG1-initiated BER, 8-oxoG base. Our results showing that 8-oxoG base exposure of cells leads to increased Rho–GTP levels raise the possibility that OGG1-BER is coupled to cellular morphological changes and the regulation of the cytoskeleton via Rho in oxidatively stressed cells. To test whether OGG1-BER and release of 8-oxoG are key events in Rho activation and changes in cytoskeleton, OGG1-initiated BER was prevented using siRNA specific for OGG1. As expected, ablation of OGG1 significantly decreased Rho activation in both oxidatively stressed and 8-oxoG-challenged cells.

In our studies, we utilized experimental animals to show the translational significance of our studies. Our rationale for using the lungs was that they

directly interact with the environment and are exposed to pollutants, resulting in oxidative stress and consequently DNA damage [48], including guanine oxidation, which is subject to repair via OGG1-BER. In addition, major age- and occupation-related chronic airway diseases (e.g., asthma and COPD) are associated with tissue remodeling, which is thought to be related to an increased oxidative state and DNA damage [49]. In 8-oxoG base-challenged mouse lungs RhoA was activated; consequently α-SMA was polymerized into the cytoskeleton and accumulated in insoluble fractions. Thus our data may give us a clue to a mechanism by which ROS-induced DNA damage and OGG1-initiated repair of oxidative DNA damage play roles in lung remodeling, and fibrosis, including idiopathic pulmonary fibrosis. These cellular pathological changes are usually linked to decreased DNA repair, including OGG1-BER. Interestingly, our findings show the opposite, the involvement of OGG1-intiated BER in cytoskeletal changes. One may propose that oxidative stress, generation of DNA base damage, and the consequent DNA repair by OGG1 could be involved in organ/tissue remodeling observed in various chronic diseases or aging-associated processes. Although it should be proven experimentally, we speculate that decreased OGG1 activity observed in fibrotic tissues and malignant cells, for example, could be a cellular defense against extensive cellular cytoskeletal changes that are required for the proliferation and migration of cancerous cells.

**Acknowledgments**

This work was supported by Grants NIEHS RO1 ES018948 (I.B.), NIA/AG 021830 (I.B.), and NIAID/AI062885 (I.B.) and the NHLBI Proteomic Center, N01HV00245 (Dr. A. Kurosky); the International Science–Technology Collaboration Foundation (20120728) of Jilin Province in China (X.B.); and the TAMOP 4.2.1/B-09/1/KONV-2010-2007 project, which is cofinanced by the European Union and the European Social Fund. A.B. was also supported by the Janos Bolyai Fellowship from the Hungarian Academy of Sciences. We thank Dr. David Konkel (Institute for Translational Sciences, UTMB) and Mardelle Susman (Microbiology and Immunology, UTMB) for their scientific input and critical editing of the manuscript.

## References


[1] Loft, S.; Hogh Danielsen, P.; Mikkelsen, L.; Risom, L.; Forchhammer, L.; Moller, P. Biomarkers of oxidative damage to DNA and repair. Biochem. Soc. Trans. 36:1071–1076; 2008.

[2] Margolin, Y.; Cloutier, J. F.; Shafirovich, V.; Geacintov, N. E.; Dedon, P. C. Paradoxical hotspots for guanine oxidation by a chemical mediator of inflammation. Nat. Chem. Biol. 2:365–366; 2006.

[3] Dizdaroglu, M.; Kirkali, G.; Jaruga, P. Formamidopyrimidines in DNA: mechanisms of formation, repair, and biological effects. Free Radic. Biol. Med. 45:1610–1621; 2008.

[4] Cooke, M. S.; Evans, M. D.; Dizdaroglu, M.; Lunec, J. Oxidative DNA damage: mechanisms, mutation, and disease. FASEB J. 17:1195–1214; 2003.

[5] Radak, Z.; Boldogh, I. 8-Oxo-7,8-dihydroguanine: links to gene expression, aging, and defense against oxidative stress. Free Radic. Biol. Med. 49:587–596; 2010.

[6] Mitra, S.; Izumi, T.; Boldogh, I.; Bhakat, K. K.; Hill, J. W.; Hazra, T. K. Choreography of oxidative damage repair in mammalian genomes. Free Radic. Biol. Med. 33:15–28; 2002.

[7] David, S.S.; O'Shea, V. L.; Kundu, S. Base-excision repair of oxidative DNA damage. Nature 447:941–950; 2007.

[8] Rosenquist, T. A.; Zharkov, D. O.; Grollman, A. P. Cloning and characterization of a mammalian 8-oxoguanine DNA glycosylase. Proc. Natl. Acad. Sci. USA 94:7429–7434; 1997.

[9] Nishimura, S. Involvement of mammalian OGG1(MMH) in excision of the 8-hydroxyguanine residue in DNA. Free Radic. Biol. Med. 32:813–821; 2002.

[10] Sassa, A.; Beard, W. A.; Prasad, R.; Wilson, S. H. DNA sequence context effects on the glycosylase activity of human 8-oxoguanine DNA glycosylase. J. Biol. Chem. 287:36702–36710; 2012.

[11] Klungland, A.; Rosewell, I.; Hollenbach, S.; Larsen, E.; Daly, G.; Epe, B.; Seeberg, E.; Lindahl, T.; Barnes, D. E. Accumulation of premutagenic DNA lesions in mice defective in removal of oxidative base damage. Proc. Natl. Acad. Sci. USA 96:13300–13305; 1999.

[12] Sakumi, K.; Tominaga, Y.; Furuichi, M.; Xu, P.; Tsuzuki, T.; Sekiguchi, M.; Nakabeppu, Y. Ogg1 knockout-associated lung tumorigenesis and its suppression by Mth1 gene disruption. Cancer Res. 63:902–905; 2003.

[13] Minowa, O.; Arai, T.; Hirano, M.; Monden, Y.; Nakai, S.; Fukuda, M.; Itoh, M.; Takano, H.; Hippou, Y.; Aburatani, H.; Masumura, K.; Nohmi, T.; Nishimura, S.; Noda, T. Mmh/Ogg1 gene inactivation results in

accumulation of 8-hydroxyguanine in mice. Proc. Natl. Acad. Sci. USA 97:4156–4161; 2000.

[14] Mabley, J. G.; Pacher, P.; Deb, A.; Wallace, R.; Elder, R. H.; Szabo, C. Potential role for 8-oxoguanine DNA glycosylase in regulating inflammation. FASEB J. 19:290–292; 2005.

[15] Sampath, H.; Vartanian, V.; Rollins, M. R.; Sakumi, K.; Nakabeppu, Y.; Lloyd, R. S. 8-Oxoguanine DNA glycosylase (OGG1) deficiency increases susceptibility to obesity and metabolic dysfunction. PLoS One 7:e51697; 2012.

[16] Conlon, K. A.; Zharkov, D. O.; Berrios, M. Cell cycle regulation of the murine 8-oxoguanine DNA glycosylase (mOGG1): mOGG1 associates with microtubules during interphase and mitosis. DNA Repair (Amsterdam) 3:1601–1615; 2004.

[17] Dantzer, F.; Luna, L.; Bjoras, M.; Seeberg, E. Human OGG1 undergoes serine phosphorylation and associates with the nuclear matrix and mitotic chromatin in vivo. Nucleic Acids Res. 30:2349–2357; 2002.

[18] Fromme, J. C.; Bruner, S. D.; Yang, W.; Karplus, M.; Verdine, G. L. Product assisted catalysis in base-excision DNA repair. Nat. Struct. Biol. 10:204–211; 2003.

[19] Boldogh, I.; Hajas, G.; Aguilera-Aguirre, L.; Hegde, M. L.; Radak, Z.; Bacsi, A.; Sur, S.; Hazra, T. K.; Mitra, S. Activation of Ras signaling pathway

by 8-oxoguanine DNA glycosylase bound to its excision product, 8-oxoguanine. J. Biol. Chem. 287:20769–20773; 2012.

[20] German, P.; Szaniszlo, P.; Hajas, G.; Radak, Z.; Bacsi, A.; Hazra, T. K.; Hegde, M. L.; Ba, X.; Boldogh, I. Activation of cellular signaling by 8-oxoguanine DNA glycosylase-1-initiated DNA base excision repair. DNA Repair (Amsterdam) 12:856–863; 2013.

[21] Hajas, G.; Bacsi, A.; Aguilera-Aguirre, L.; Hegde, M. L.; Tapas, K. H.; Sur, S.; Radak, Z.; Ba, X.; Boldogh, I. 8-Oxoguanine DNA glycosylase-1 links DNA repair to cellular signaling via the activation of the small GTPase Rac1. Free Radic. Biol. Med. 61C:384–394; 2013.

[22] Soza, S.; Leva, V.; Vago, R.; Ferrari, G.; Mazzini, G.; Biamonti, G.; Montecucco, A. DNA ligase I deficiency leads to replication-dependent DNA damage and impacts cell morphology without blocking cell cycle progression. Mol. Cell. Biol. 29:2032–2041; 2009.

[23] Giry, M.; Popoff, M. R.; von Eichel-Streiber, C.; Boquet, P. Transient expression of RhoA, -B, and -C GTPases in HeLa cells potentiates resistance to Clostridium difficile toxins A and B but not to Clostridium sordellii lethal toxin. Infect. Immun. 63:4063–4071; 1995.

[24] Boldogh, I.; Bacsi, A.; Choudhury, B. K.; Dharajiya, N.; Alam, R.; Hazra, T. K.; Mitra, S.; Goldblum, R. M.; Sur, S. ROS generated by pollen NADPH

oxidase provide a signal that augments antigen-induced allergic airway inflammation. J. Clin. Invest. 115:2169–2179; 2005.

[25] Reid, T.; Furuyashiki, T.; Ishizaki, T.; Watanabe, G.; Watanabe, N.; Fujisawa, K.; Morii, N.; Madaule, P.; Narumiya, S. Rhotekin, a new putative target for Rho bearing homology to a serine/threonine kinase, PKN, and rhophilin in the rho- binding domain. J. Biol. Chem. 271:13556–13560; 1996.

[26] Zhang, B.; Zhang, Y.; Wang, Z.; Zheng, Y. The role of $Mg^{2+}$ cofactor in the guanine nucleotide exchange and GTP hydrolysis reactions of Rho family GTP- binding proteins. J. Biol. Chem. 275:25299–25307; 2000.

[27] Liu, T.; Guevara, O. E.; Warburton, R. R.; Hill, N. S.; Gaestel, M.; Kayyali, U. S. Regulation of vimentin intermediate filaments in endothelial cells by hypoxia. Am. J. Physiol. Cell Physiol 299:C363–C373; 2010.

[28] Katoh, K.; Kano, Y.; Masuda, M.; Onishi, H.; Fujiwara, K. Isolation and contraction of the stress fiber. Mol. Biol. Cell 9:1919–1938; 1998.

[29] Das, S.; Chattopadhyay, R.; Bhakat, K. K.; Boldogh, I.; Kohno, K.; Prasad, R.; Wilson, S. H.; Hazra, T. K. Stimulation of NEIL2-mediated oxidized base excision repair via YB-1 interaction during oxidative stress. J. Biol. Chem. 282:28474–28484; 2007.

[30] Wheeler, A. P.; Ridley, A. J. Why three Rho proteins? RhoA, RhoB, RhoC, and cell motility Exp. Cell Res. 301:43–49; 2004.

[31] Rossman, K. L.; Der, C. J.; Sondek, J. GEF means go: turning on RHO GTPases with guanine nucleotide-exchange factors. Nat. Rev. Mol. Cell Biol. 6:167–180; 2005.

[32] Hinz, B.; Mastrangelo, D.; Iselin, C. E.; Chaponnier, C.; Gabbiani, G. Mechanical tension controls granulation tissue contractile activity and myofibroblast differentiation. Am. J. Pathol. 159:1009–1020; 2001.

[33] Uehata, M.; Ishizaki, T.; Satoh, H.; Ono, T.; Kawahara, T.; Morishita, T.; Tamakawa, H.; Yamagami, K.; Inui, J.; Maekawa, M.; Narumiya, S. Calcium sensitization of smooth muscle mediated by a Rho-associated protein kinase in hypertension. Nature 389:990–994; 1997.

[34] Shao, C.; Xiong, S.; Li, G. M.; Gu, L.; Mao, G.; Markesbery, W. R.; Lovell, M. A. Altered 8-oxoguanine glycosylase in mild cognitive impairment and late-stage Alzheimer's disease brain. Free Radic. Biol. Med. 45:813–819; 2008.

[35] Kaneko, T.; Tahara, S.; Matsuo, M. Non-linear accumulation of 8-hydroxy-2'- deoxyguanosine, a marker of oxidized DNA damage, during aging. Mutat. Res. 316:277–285; 1996.

[36] Markesbery, W. R.; Lovell, M. A. DNA oxidation in Alzheimer's disease. Antioxid. Redox Signaling 8:2039–2045; 2006.

[37] Wilson, D.M., 3rd; Bohr, V.A. The mechanics of base excision repair, and its relationship to aging and disease. DNA Repair (Amsterdam) 6:544–559; 2007.

[38] Hegde, M. L.; Mantha, A. K.; Hazra, T. K.; Bhakat, K. K.; Mitra, S.; Szczesny, B. Oxidative genome damage and its repair: implications in aging and neurodegenerative diseases. Mech. Ageing Dev. 133:157–168; 2012.

[39] Gourlay, C. W.; Ayscough, K. R. The actin cytoskeleton: a key regulator of apoptosis and ageing? Nat. Rev. Mol. Cell Biol. 6:583–589; 2005.

[40] Heo, J.; Raines, K. W.; Mocanu, V.; Campbell, S. L. Redox regulation of RhoA. Biochemistry 45:14481–14489; 2006.

[41] Aghajanian, A.; Wittchen, E. S.; Campbell, S. L.; Burridge, K. Direct activation of RhoA by reactive oxygen species requires a redox-sensitive motif. PLoS One 4: e8045; 2009.

[42] Van Aelst, L.; D'Souza-Schorey, C. Rho GTPases and signaling networks. Genes Dev. 11:2295–2322; 1997.

[43] Bourne, H. R.; Sanders, D. A.; McCormick, F. The GTPase superfamily: a conserved switch for diverse cell functions. Nature 348:125–132; 1990.

[44] Boriack-Sjodin, P. A.; Margarit, S. M.; Bar-Sagi, D.; Kuriyan, J. The structural basis of the activation of Ras by Sos. Nature 394:337–343; 1998.

[45] Bickle, M.; Delley, P. A.; Schmidt, A.; Hall, M. N. Cell wall integrity modulates RHO1 activity via the exchange factor ROM2. EMBO J. 17:2235–2245; 1998.

[46] Schmidt, A.; Hall, A. Guanine nucleotide exchange factors for Rho GTPases: turning on the switch. Genes Dev. 16:1587–1609; 2002.

[47] Kis, K.; Liu, X.; Hagood, J. S. Myofibroblast differentiation and survival in fibrotic disease. Expert Rev. Mol. Med. 13:e27; 2011.

[48] Kinnula, V. L.; Crapo, J. D. Superoxide dismutases in the lung and human lung diseases. Am. J. Respir. Crit. Care Med. 167:1600–1619; 2003.

[49] Faner, R.; Rojas, M.; Macnee, W.; Agusti, A. Abnormal lung aging in chronic obstructive pulmonary disease and idiopathic pulmonary fibrosis. Am. J. Respir. Crit. Care Med. 186:306–313; 2012.

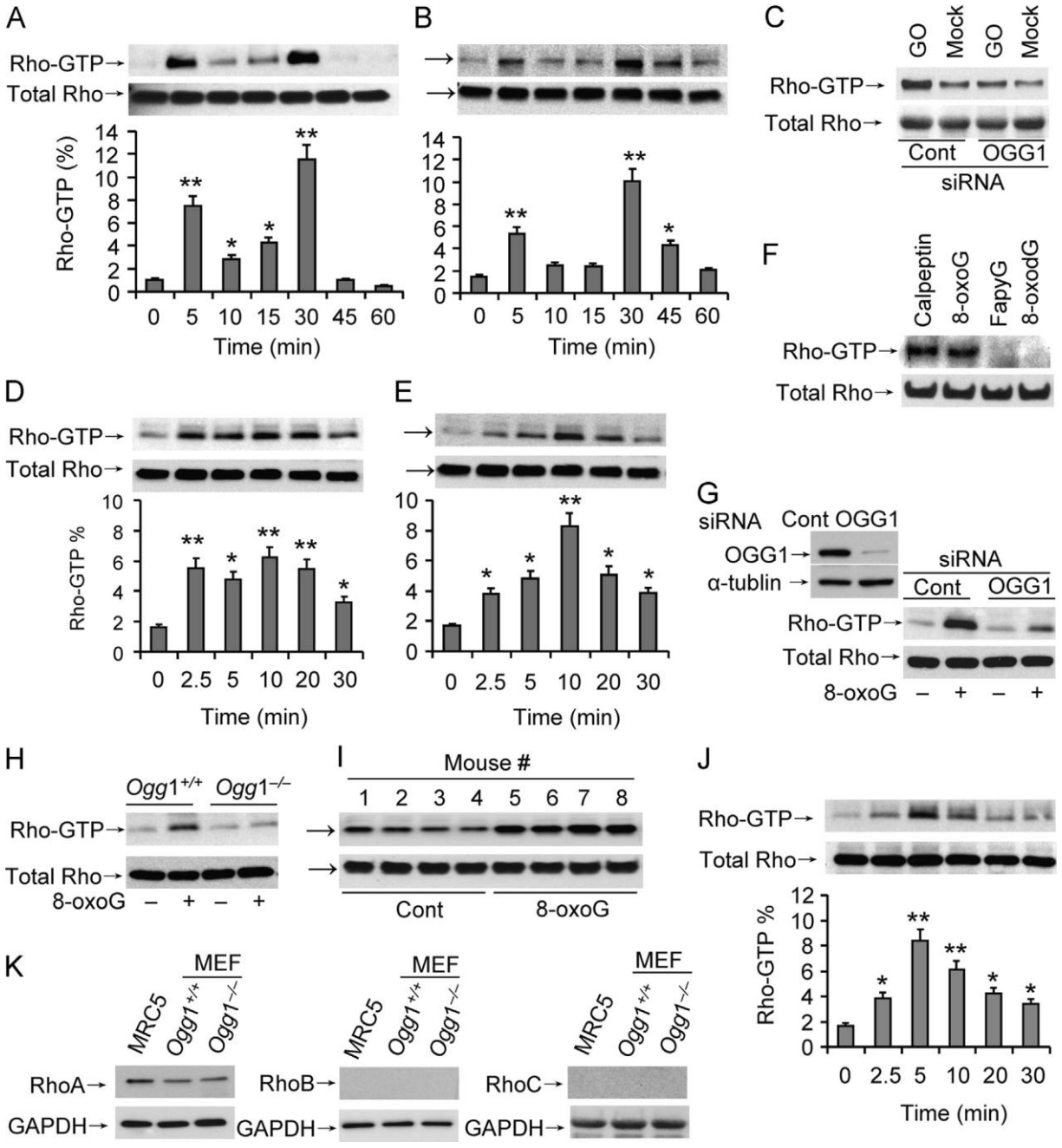


Fig. 1. Activation of Rho GTPase coincides with OGG1-initiated BER. (A, B) Increased Rho–GTP levels in cultured cells exposed to oxidative stress. (A) MRC-5 and (B) MEF cells were exposed to GOx (100 ng/ml) and lysed at the times indicated. Rho–GTP levels were determined in 500 μg cell extracts by active Rho pull-down assays. (C) OGG1 depletion decreased Rho activation. MRC5 cells were transfected with siRNA to OGG1 or control siRNA and exposed to GO for 5 min. Rho–GTP was determined as for (A) and (B). (D, E) The OGG1-BER product 8-oxoG base increases Rho–GTP levels. (D) MRC5 and (E) MEF cells were exposed to 8-oxoG (10 μM) at 37 °C, cell extracts prepared at the indicated times, and Rho–

GTP levels determined as for (A) and (B). (F) Lack of Rho activation in FapyG-exposed cells. Cells were exposed to FapyG (10 μM) and cell extracts were prepared at 5 min and Rho–GTP levels determined as for (A) and (B). As controls, calpeptin (a Rho activator) and 8-oxodG were used. (G) OGG1 depletion prevents Rho activation in 8-oxoG-exposed cells. MRC5 cells were transfected with OGG1 or control siRNA and exposed to 8-oxoG for 5 min. Rho–GTP was determined as for (A) and (B). Inset: extent of OGG1 downregulation by siRNA. (H) Lack of 8-oxoG-induced Rho activation in $Ogg^{-/-}$ MEFs. Cells ($Ogg1^{-/-}$ and $Ogg1^{+/+}$) were challenged with 8-oxoG, extracts were made at 5 min, and changes in Rho–GTP levels were determined by pull-down assays as for (A) and (B). (I) Activation of Rho GTPase in mouse lungs. Mice were challenged with 8-oxoG (1 mM) via the intranasal route and at 30 min active Rho was determined by pull-down assays. (J) Activation of Rho in lung extracts by 8-oxoG. Lung extracts from unchallenged mice were incubated with 10 mM 8-oxoG as indicated and changes in Rho–GTP levels determined as for (A) and (B). The graphs in (A), (B), (D), (E), and (J) depict the % of activated Rho. Band intensities were analyzed with ImageJ software and the percentage of active Rho in total Rho was calculated. (K) Expression of Rho isotypes in MRC-5 and $Ogg1^{-/-}$ and $Ogg1^{+/+}$ MEF cells. Cell extracts (20 μg) were subjected to SDS–PAGE and RhoA, B, and C levels were determined by immunoblotting using type-specific Abs. GAPDH levels show equal loading. Cont, control. MEF, mouse embryonic fibroblasts; MRC5, human embryonic lung fibroblasts. Each experiment was repeated at least three times. $^{*}p < 0.05$, $^{**}p < 0.01$.

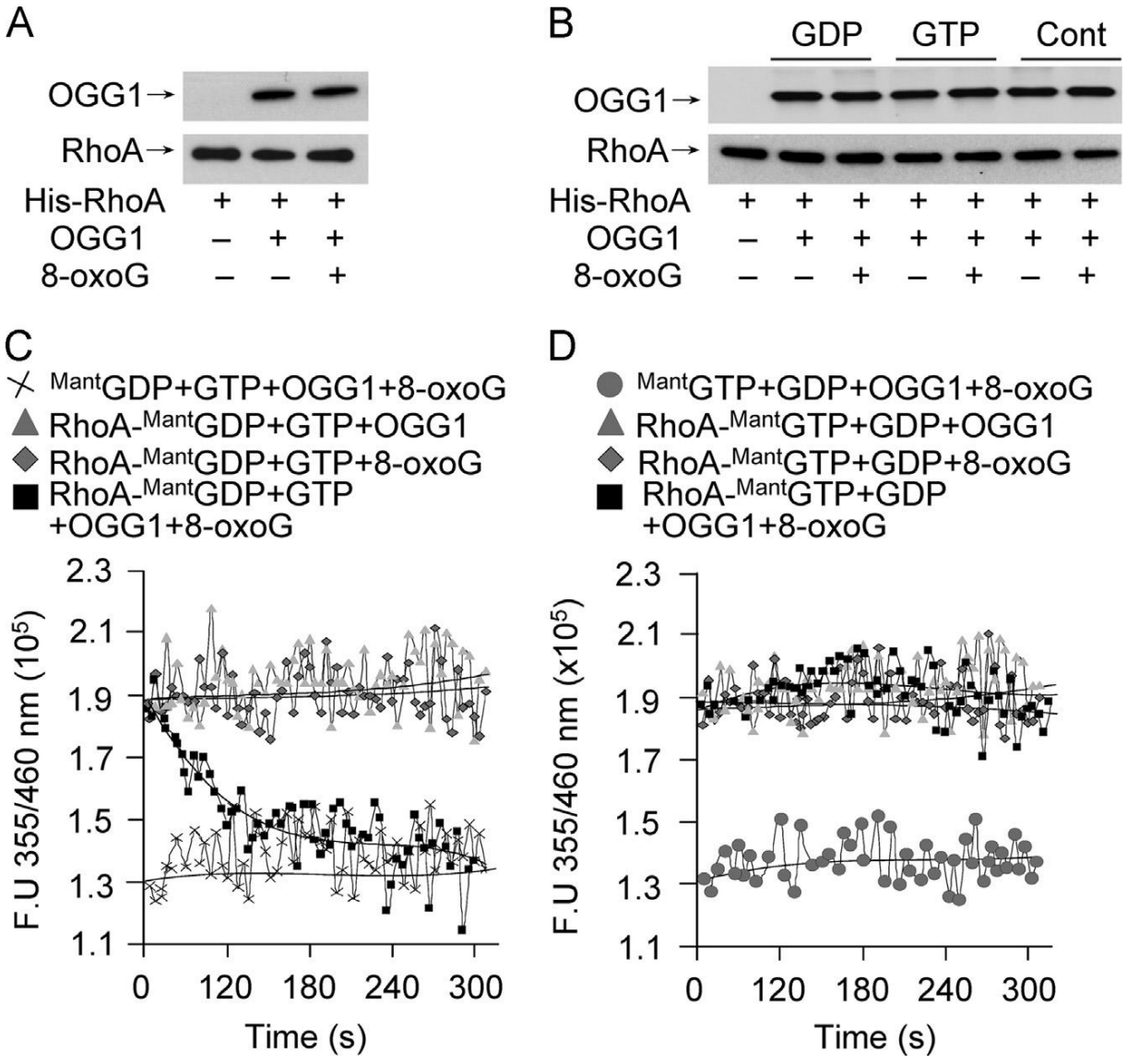


Fig. 2. Interaction of OGG1 with RhoA protein and guanine nucleotide exchange in the presence of 8-oxoG base. (A) Physical interaction of OGG1 protein with RhoA. His-RhoA (6 pmol) bound to Ni–NTA was incubated with OGG1 protein (6 pmol) for 30 min ± 8-oxoG (6 pmol). OGG1 binding to Rho was detected by Western blot analysis. (B) Physical interaction of OGG1 protein with RhoA in the presence of GDP, GTP, and/or 8-oxoG was detected as described for (A). (C) Exchange of RhoA-bound GDP to GTP by OGG1 in the presence of the 8-oxoG base. RhoA protein (6 pmol) was loaded with $^{Mant}$GDP (6 pmol) and nucleotide exchange was initiated by adding OGG1 + 8-oxoG and GTP (6 pmol) (■). The controls, RhoA–$^{Mant}$GDP + GTP + OGG1, RhoA–$^{Mant}$GDP + GTP + 8-oxoG, or $^{Mant}$GDP + GTP + OGG1 + 8-oxoG, did not catalyze RhoA–GTP → GDP exchange. (D) OGG1 does not catalyze RhoA–GTP → GDP exchange. RhoA loaded with $^{Mant}$GTP was incubated

with GDP + OGG1 + 8-oxoG, GDP + 8-oxoG, or GDP + OGG1. The control was $^{Mant}$GTP with GDP + OGG1 + 8-oxoG. In (C) and (D), changes in the fluorescence of RhoA–$^{Mant}$GDP and RhoA–$^{Mant}$GTP were determined by real-time measurements using a POLARstar Omega (BMG Labtech). Curves were fitted using MS Excel, n = 3–5.

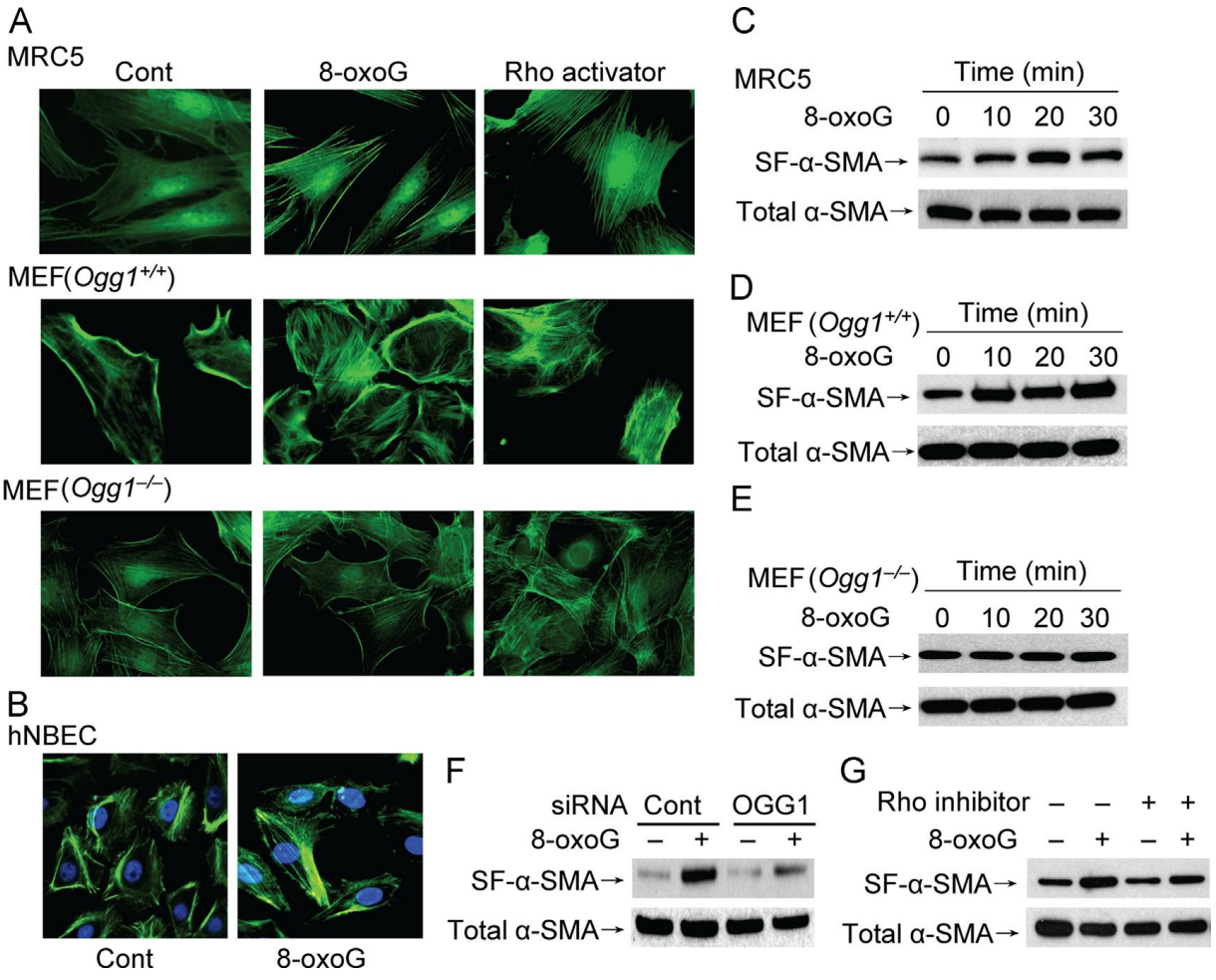


Fig. 3. α-SMA polymerization into stress fibers in OGG1-expressing cells. (A) MRC5 and MEF cells and (B) hNBECs were challenged with 8-oxoG (10 mM) for 20 min, fixed, and stained with FITC–phalloidin. Representative images were taken using a Nikon Eclipse Ti microscope system ( x 192 original magnification). As a positive control, cells were incubated with the Rho activator calpeptin (1 unit/ml) for 20 min. (C–E) Cells were treated with 8-oxoG (10 mM) for the indicated times and insoluble fractions were isolated as described under Materials and methods. α-SMA polymerized into stress fibers was detected by Western blot analysis. (F) MRC5 cells were transfected with OGG1-specific or control siRNA as described under Materials and methods, and α-SMA in stress fibers was examined 20 min after challenge with 8-oxoG. (G) MRC5 cells were incubated with the Rho inhibitor C3 transferase (2 μg/ml) for 4 h before a 20-min 8-oxoG challenge. Insoluble fractions were isolated and α-SMA in the isolated fractions was analyzed by Western blotting. SF-α-SMA, α-SMA in the stress fibers; Cont, control; hNBEC, human normal bronchial epithelial cell; FITC, fluorescein isothiocyanate. Each experiment was repeated at least three times.

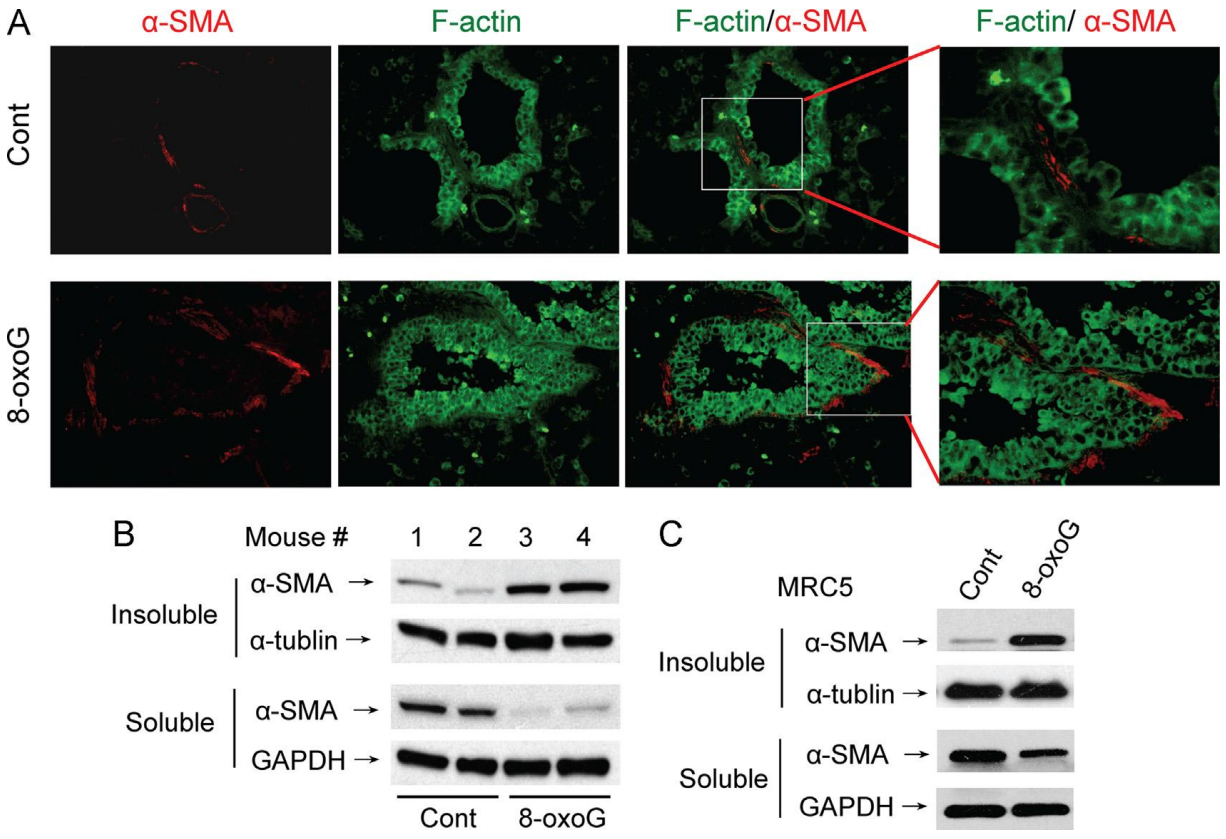


Fig. 4. 8-OxoG base-induced α-SMA polymerization in lungs. (A) Lungs were 8-oxoG (1 mM)-challenged and excised 30 min thereafter, fixed, sectioned, and stained with antibody to α-SMA (red) and F-actin (green). Images were taken using a Nikon Eclipse Ti microscope system ( x 138 original magnification). (B) Lungs were excised and the trachea and bronchial branches removed and homogenized in cytoskeleton lysis buffer. Triton X-100-insoluble (cytoskeletal) and soluble fractions were subjected to PAGE. α-SMA (and α-tubulin and GAPDH used as loading controls) was detected using specific antibodies. (C) MRC5 cells were exposed to 8-oxoG (10 mM) for 20 min and Triton X-100-insoluble and soluble fractions were analyzed as for (B). Cont, control. Each experiment was repeated at least three times.